toxic effects originally attributed to NO are now considered to be mediated mostly by the compound peroxynitrite [2]. Thus, in the present study, we tested the hypothesis that ebselen, a glutathione peroxidase mimic and a scavenger of peroxynitrite, attenuates noise-induced excitotoxicity and TTS.

Twenty-four male albino guinea pigs (250–350 g), with normal auditory brainstem response (ABR) thresholds at 2, 4, 8 and 16 kHz, were randomly divided into vehicle-treated ($n=14$) and ebselen-treated experimental groups ($n=10$). These animals received an oral dose of 0.25 ml of 99% chloroform solution alone (vehicle) or containing 10 mg/kg ebselen one hour before exposure to noise. Ten mg/kg of ebselen was selected because this dose most effectively attenuates PTS in guinea pigs [13]. The animals were subjected to a 3-h noise exposure (115 dB SPL, 4-kHz octave band noise) generated within a single-walled, sound-deadened chamber. Two separately caged animals were tested at one time and allowed to move freely during exposure. The sound chamber was fitted with speakers driven by a noise generator and power amplifier. A 0.5-in. Bruel and Kjaer condenser microphone and a fast Fourier transform analyzer were used to measure and calibrate the sound level at various locations within the chamber to ensure stimulus uniformity within ±1 dB.

Five animals in each group underwent ABR measurements immediately and 1, 3, 7, and 14 days after noise exposure to assess the effect of ebselen on TTS. The method of ABR measurement has been described previously [13]. In brief, animals were anesthetized with a mixture of xylazine hydrochloride (10 mg/kg, i.m.) and ketamine hydrochloride (40 mg/kg, i.m.), and needle electrodes were placed subcutaneously at the vertex (active electrode), beneath the pinna of the measured ear (reference electrode), and beneath the opposite ear (ground). The stimulus duration was 15 ms; the presentation rate, 11/s; and the rise/fall time, 1 ms. Responses of 1024 sweeps were averaged at each intensity level (5 dB steps) to assess threshold. Threshold was defined as the lowest intensity level at which a clear reproducible waveform was visible in the trace.

Four animals given vehicle alone were euthanized under deep anesthesia with xylazine hydrochloride and ketamine hydrochloride 7 days after noise exposure to assess hair cell damage. Two animals unexposed to noise served as controls. The cochleae were perfused intrascalarly with 4% paraformaldehyde and immersed in the same fixative overnight. The surface of the organ of Corti was stained with rhodamine phalloidin and each turn of the cochlea was observed under fluorescent microscope as previously described [13]. The influence of ebselen on noise-induced morphological changes in the cochlea was examined in the remaining animals ($n=5$ in each group). These animals were deeply anesthetized with a mixture of xylazine hydrochloride and ketamine hydrochloride immediately after the termination of noise exposure. The left bulla was then exposed and the perilymphatic spaces perfused for 10 min with 2% paraformaldehyde in 2.5% glutaraldehyde. The animals were then sacrificed and the left cochlea quickly removed, immersed in the same fixative for 24 h, and decalcified in 10% ethylenediaminetetraacetic acid for 14 days. The specimens were post-fixed in 1% osmium tetroxide for 2 h, dehydrated in a graded series of ethanol, and embedded in epoxy resin. Ultra-thin sections were obtained from the very upper part of the basal turn corresponding to the region most responsive to frequencies in the range of 4–6 kHz and observed under transmission electron microscope (TEM). We focused on the histological changes in the stria vascularis, the hair cells and supporting cells, and the afferent dendrites beneath the IHCs. Because the extent of swelling of the afferent dendrites was obviously different between vehicle- and ebselen-treated animals, we compared the area (μm^2) of the swollen dendrites in the two groups. In each animal, a total of 10 sections that contained the nucleus of different IHC were collected. From these, five sections were chosen randomly for measuring and statistical analysis by a blinded technician who did not know the aim of the current study. The images of these sections were captured using a scanner, the area of the swollen dendrites measured using Adobe Photoshop image analysis software, and the mean of the areas calculated. Student's t-test was used for statistical analysis.

The experimental protocol was approved by the University Committee for the Use and Care of Animals at the University of Tokyo and conforms to the National Institute of Health Guide for the Care and Use of Laboratory Animals.

ABR thresholds before noise exposure were essentially equivalent among all animals. In vehicle-treated controls, ABR thresholds were moderately increased immediately after noise; the threshold shifts were approximately 25 dB at 2 kHz and 45 dB at 4, 8, and 16 kHz. The ABR thresholds then showed gradual recovery, returning to pre-exposure baseline thresholds 7 days later, indicating that the noise exposure induced a TTS. In contrast, ebselen-treated animals showed virtually no ABR threshold shifts after noise (Fig. 1). The ABR thresholds shifts immediately after noise were significantly different ($p<0.001$) at all frequencies measured between control and ebselen-treated animals. The IHCs and outer hair cells (OHCs) were well preserved in both vehicle-treated noise-exposed animals and unexposed controls; the number of missing OHCs in the lower two turns was 6.4 ± 2.5 in the former and 4.9 ± 4.4 in the latter, suggestive that the noise used did not cause hair cell death.

In controls that were euthanized immediately after noise, the OC in the upper basal turn showed numerous swollen dendrites beneath the IHCs. In contrast, pathological changes were quite limited in ebselen-treated animals (Fig. 2). The mean area of swollen dendrites was significantly smaller ($p<0.01$) in ebselen-treated animals compared to controls. In neither controls or ebselen-treated animals sacrificed immediately after noise exposure was there obvious evidence of other pathological changes reported to be correlated to TTS, such as edema or vasoconstriction in the stria vascularis, buckling of the pillar bodies, or fusion or loss of stereocilia.

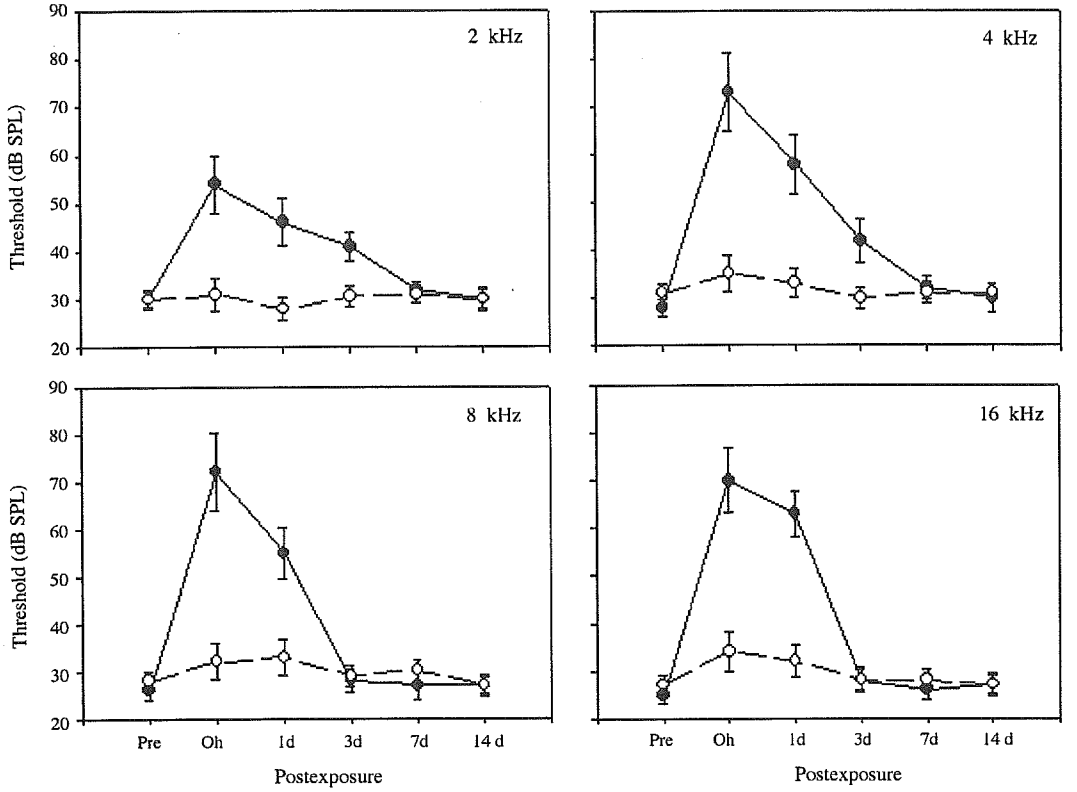

Fig. 1. Thresholds of auditory brainstem response (mean ± S.D.) measured before and immediately and 1, 3, 7, and 14 days following noise exposure in vehicle-treated controls (●) and ebselen-treated animals (○).

The current study shows that ebselen virtually prevents noise-induced TTS under conditions where vehicle-treated controls developed a TTS of approximately 25–45 dB. TEM observation revealed that immediately after noise, the afferent dendrites beneath the IHCs were severely swollen in control animals, whereas such pathological changes were significantly reduced in ebselen-treated animals. Other pathological changes were not evident in either controls or ebselen-treated animals. Because we did not examine otoacoustic emissions or use scanning electron microscopy, it is possible that functional and/or subtle anatomical changes in the regions other than the afferent dendrite, especially the OHCs, were missed. However, the above findings indicate that ebselen can attenuate noise-induced changes at least in the afferent dendrites beneath the IHCs and thereby TTS.

Using fluorescent dye 4,5-diaminofluorescein diacetate, it has been shown that in the normal guinea pig cochlea, NO is present in the afferent nerves and their putative endings near the IHCs, putative efferent nerve endings near the OHCs, the IHCs and OHCs, and blood vessels [20], and that inducible NO synthase (iNOS) is expressed in cochlear nerve fibers, as well as in hair cell stereocilia, Hensen's cells, and the stria vascularis [19]. It has also been reported that, when exposed to broadband noise (3 h/day at 110 or 120 dB SPL) for three consecutive days, NO concentration is increased in the perilymph, NO fluorescence becomes more intense in the IHCs and OHCs [21], and iNOS fluorescence signals becomes more intense in cochlear tissues compared to unexposed controls [19]. In addition, it has been reported that cochlear perfusion with kainic acid (KA), a conformationally restricted analog of glutamate known to have excitotoxic effects on spiral ganglion cells, causes significant elevation of thresholds of the cochlear nerve compound action potential and that this threshold shift is significantly reduced by pretreatment with nitroindazole, a competitive inhibitor of neuronal NOS [6]. The toxic effects originally attributed to NO are now regarded to be mediated mostly by the compound peroxynitrite [2]. Considering these findings, it is likely that ebselen attenuated noise-induced excitotoxicity and thereby TTS, by scavenging peroxynitrite formed by the reaction between noise-induced $O_2^{\bullet -}$ and NO.

It may also be possible that ebselen attenuated TTS because of its antioxidant property. It has been shown, however, that topical application of R-PIA, which increases endogenous antioxidant levels, to the chinchilla cochlea facilitates the recovery of hearing function 4 days after noise exposure but does not attenuate initial noise-induced threshold shifts [5]. Ohinata et al. [10] have shown that lipid peroxidation (8-isoprostane formation) in the OC induced by intense noise is significantly attenuated by *N*-methyl-D-aspartate (NMDA) receptor antagonists and anti-oxidant *N*-acetylcysteine, but not by NOS inhibitor, L-*N* (omega)-nitroarginine methyl

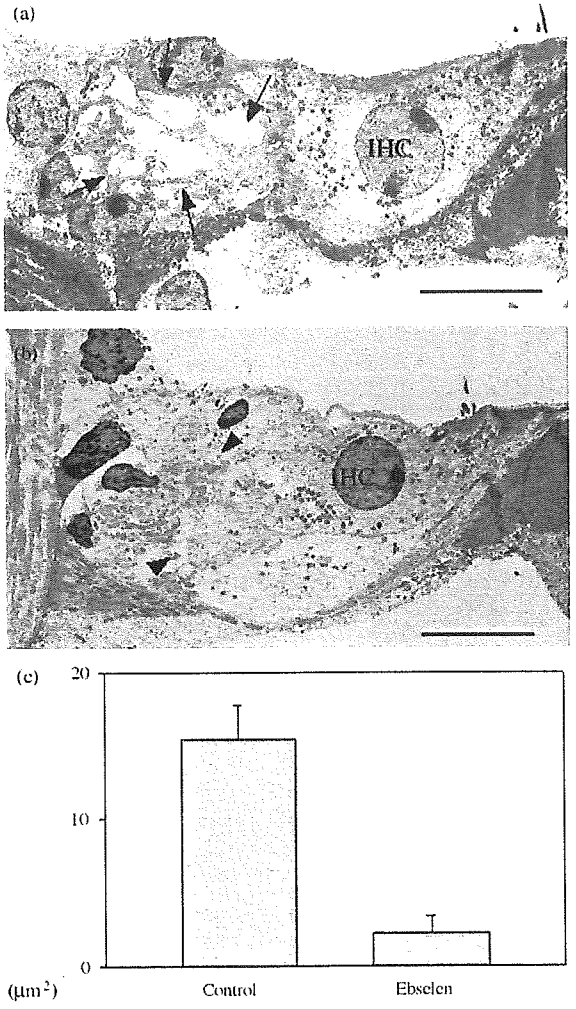

Fig. 2. Typical transmission electron microscopic findings in the medial side of the organ of Corti immediately following noise exposure in vehicle-treated controls (a) and ebselen-treated animals (b). The afferent dendrites are markedly swollen in vehicle-treated controls (arrows) but relatively normal in ebselen-treated animals (arrowheads). The bar indicates 10 μm; IHC: inner hair cell. (c) The mean ± S.D. of areas (μm^2) of the swollen afferent dendrites in the vehicle-treated control and ebselen-treated animals.

ester. Therefore, it is unlikely that ebselen's protective effect against TTS is provided chiefly by scavenging ROS or reducing ROS formation in the OC.

In conclusion, the current study shows that ebselen can prevent noise-induced excitotoxicity and thereby TTS. This prevention likely reflects ebselen's scavenging of peroxynitrite, thus supporting the view that peroxynitrite, at least in part, mediates excitotoxicity induced by intense noise. It has previously been shown that ebselen can also attenuate PTS in guinea pigs [13] and rats [7]. Since ebselen has already been used in humans clinically to treat ischemic stroke with few or no side effects [12], our findings reinforce the potential clinical utility of ebselen to prevent and/or treat noise-induced hearing loss in humans.

Acknowledgements

We thank Prof. J.M. Miller, Kresge Hearing Research Institute, University of Michigan, for helpful comments and discussion and Mr. Y. Mori for technical support. This work was supported by a grant (15110201) from the Ministry of Health, Labour and Welfare, Japan to T.Y., and a grant (13470357) from the Ministry of Education, Culture, Sports, Science and Technology, Japan to T.Y.

References

[1] W.W. Clark, Recent studies of temporary threshold shift (TTS) and permanent threshold shift (PTS) in animals, J. Acoust. Soc. Am. 90 (1991) 155–163.
[2] J.P. Crow, J.S. Beckman, The role of peroxynitrite in nitric oxide mediated toxicity, Curr. Top. Microbiol. Immunol. 196 (1995) 53–73.
[3] V.L. Dawson, T.M. Dawson, E.D. London, D.S. Bredt, S.H. Snyder, Nitric oxide mediates glutamate neurotoxicity in primary cortical cultures, Proc. Natl. Acad. Sci. U.S.A. 88 (1991) 6368–6371.
[4] D. Henderson, S.L. McFadden, C.C. Liu, N. Hight, X.Y. Zheng, The role of antioxidants in protection from impulse noise, Ann. N. Y. Acad. Sci. 884 (1999) 368–380.
[5] B.H. Hu, X.Y. Zheng, S.L. McFadden, R.D. Kopke, D. Henderson, *R*-Phenylisopropyladenosine attenuates noise-induced hearing loss in the chinchilla, Hear. Res. 113 (1997) 198–206.
[6] K.L. Johnson, V. Carrasco, J. Prazma, C.J. Zdanski, W.F. Durland, H.C. Pillsbury, Role of nitric oxide in kainic acid-induced elevation of cochlear compound action potential thresholds, Acta Otolaryngol. (Stockh.) 118 (1998) 660–665.
[7] E.D. Lynch, R. Gu, C. Pierce, J. Kil, Ebselen-mediated protection from single and repeated noise exposure in rat, Laryngoscope 114 (2004) 333–337.
[8] P.R. Montague, C.D. Gancayco, M.J. Winn, R.B. Marchase, M.J. Friedlander, Role of NO production in NMDA receptor-mediated neurotransmitter release in cerebral cortex, Science 263 (1994) 973–977.
[9] A.S. Nordman, B.A. Bohne, G.W. Harding, Histopathological differences between temporary and permanent threshold shift, Hear. Res. 139 (2000) 13–30.
[10] Y. Ohinata, J.M. Miller, J. Schacht, Protection from noise-induced lipid peroxidation and hair cell loss in the cochlea, Brain Res. 966 (2003) 265–273.
[11] O.P. Ottersen, Y. Takumi, A. Matsubara, A.S. Landsend, J.H. Laake, S. Usami, Molecular organization of a type of peripheral glutamate synapse: the afferent synapses of hair cells in the inner ear, Prog. Neurobiol. 54 (1998) 127–148.
[12] M.J. Parnham, H. Sies, Ebselen: prospective therapy for cerebral ischemia, Exp. Opin. Investig. Drugs 9 (2000) 607–619.
[13] A. Pourbakht, T. Yamasoba, Ebselen attenuates cochlear damage caused by acoustic trauma, Hear. Res. 181 (2003) 100–108.
[14] J.L. Puel, C. Gervais d'Aldin, S. Saffiedine, M. Eybalin, R. Pujol, Excitotoxicity and plasticity of IHC—auditory nerve contributes to both temporary and permanent threshold shift, in: A. Axelsson, H.M. Borchgrevink, R.P. Hamernik, P.A. Hellström, D. Henderson, R.L. Salvi (Eds.), Scientific Basis of Noise-induced Hearing Loss, Thieme, New York, 1996, pp. 36–42.
[15] J.L. Puel, S. Saffiedine, C. Gervais d'Aldin, M. Eybalin, R. Pujol, Synaptic regeneration and functional recovery after excitotoxic injury in the guinea pig cochlea, C. R. Acad. Sci. III 318 (1995) 67–75.
[16] R. Pujol, J.L. Puel, Excitotoxicity, synaptic repair, and functional recovery in the mammalian cochlea: a review of recent findings, Ann. N. Y. Acad. Sci. 884 (1999) 249–254.

[17] D. Robertson, Functional significance of dendrite swelling after loud sounds in the guinea pig cochlea, Hear. Res. 9 (1983) 263–278.
[18] J.C. Saunders, E.C. Yale, Y.M. Szmyko, The structural and functional consequences of acoustic injury in the cochlea and peripheral auditory system: a five year update, J. Acoust. Soc. Am. 90 (1991) 136–146.
[19] X. Shi, C. Dai, A.L. Nuttall, Altered expression of inducible nitric oxide synthase (iNOS) in the cochlea, Hear. Res. 177 (2003) 43–52.
[20] X. Shi, T. Ren, A.L. Nuttall, Nitric oxide distribution and production in the guinea pig cochlea, Hear. Res. 153 (2001) 23–31.
[21] X. Shi, T. Ren, A.L. Nuttall, The electrochemical and fluorescence detection of nitric oxide in the cochlea and its increase following loud sound, Hear. Res. 164 (2002) 49–58.

Reprint Series

Science

15 July 2005

Vol. 309 No. 5733
Pages 337–520 $10

The Trypanosomatid Genomes

125 YEARS OF GLOBAL Science

AAAS

Mitochondrial DNA Mutations, Oxidative Stress, and Apoptosis in Mammalian Aging

G. C. Kujoth,[1] A. Hiona,[2] T. D. Pugh,[3] S. Someya,[4] K. Panzer,[1] S. E. Wohlgemuth,[2] T. Hofer,[2] A. Y. Seo,[2] R. Sullivan,[5] W. A. Jobling,[6] J. D. Morrow,[7] H. Van Remmen,[8] J. M. Sedivy,[6] T. Yamasoba,[9] M. Tanokura,[4] R. Weindruch,[3] C. Leeuwenburgh,[2] T. A. Prolla[1]*

Mutations in mitochondrial DNA (mtDNA) accumulate in tissues of mammalian species and have been hypothesized to contribute to aging. We show that mice expressing a proofreading-deficient version of the mitochondrial DNA polymerase γ (POLG) accumulate mtDNA mutations and display features of accelerated aging. Accumulation of mtDNA mutations was not associated with increased markers of oxidative stress or a defect in cellular proliferation, but was correlated with the induction of apoptotic markers, particularly in tissues characterized by rapid cellular turnover. The levels of apoptotic markers were also found to increase during aging in normal mice. Thus, accumulation of mtDNA mutations that promote apoptosis may be a central mechanism driving mammalian aging.

Mitochondria are the main source of cellular adenosine triphosphate and play a central role in a variety of cellular processes. These include fatty acid β-oxidation, phospholipid biosynthesis, calcium signaling, reactive oxygen species (ROS) generation, and apoptosis. Because the mitochondrion contains its own ~16-kilobase circular DNA, a central role for mtDNA mutations in aging has been postulated (*1*, *2*). Indeed, mtDNA mutations have been shown to accumulate with aging in several tissues of various species (*3*–*7*). The causal role of mtDNA mutations in mammalian aging is supported by a recent study demonstrating that mice with a mitochondrial mutator phenotype develop several aging phenotypes (*8*). Here, we used similar mice to investigate the cellular mechanisms by which mtDNA mutations contribute to aging.

We cloned the mouse POLG locus, *PolgA*, and used gene targeting in embryonic stem cells to introduce an AC → CT two-base substitution that corresponds to positions 1054 and 1055 of the *PolgA* cDNA (fig. S1) (*9*). This mutation results in a critical residue substitution in the conserved exonuclease domain of POLG, impairing its proofreading ability (*8*). Germline transmission of the mutation produced $PolgA^{D257A/+}$ mice, which were intercrossed to generate homozygous $PolgA^{D257A/D257A}$ mice, hereafter denoted D257A. Young D257A mice were indistinguishable from wild-type littermates, but long-term follow-up revealed a striking premature aging phenotype beginning at ~9 months of age, consisting of hair loss, graying, and kyphosis (Fig. 1, A and B). The mutant mice had a reduced life span (for

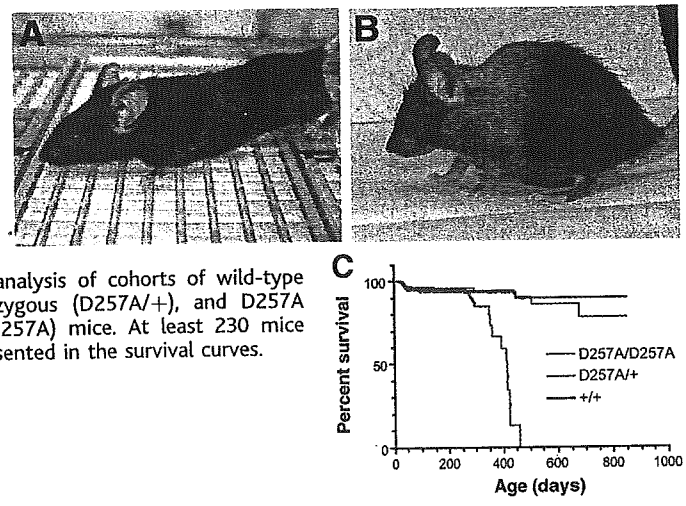

Fig. 1. D257A mice display a premature aging phenotype. Shown are wild-type (A) and D257A mice (B) at ~13 months of age. Progeroid features, including hair loss, graying, and kyphosis, become apparent at ~9 months of age. (C) Kaplan-Meier survival analysis of cohorts of wild-type (+/+), D257A heterozygous (D257A/+), and D257A homozygous (D257A/D257A) mice. At least 230 mice per genotype are represented in the survival curves.

[1]Departments of Genetics and Medical Genetics, University of Wisconsin, Madison, WI 53706, USA. [2]Department of Aging and Geriatric Research, College of Medicine, Institute on Aging, Biochemistry of Aging Laboratory, University of Florida, Gainesville, FL 32610-0107, USA. [3]Department of Medicine and Veterans Administration Hospital, University of Wisconsin, Madison, WI 53705-2286, USA. [4]Department of Applied Biological Chemistry, University of Tokyo, Bunkyo-ku, Tokyo 113-8657, Japan. [5]Waisman Center, University of Wisconsin, Madison, WI 53705-2280, USA. [6]Department of Molecular Biology, Cell Biology and Biochemistry and Center for Genomics and Proteomics, Brown University, Providence, RI 02912, USA. [7]Departments of Medicine and Pharmacology, Vanderbilt University School of Medicine, Nashville, TN 37232, USA. [8]Department of Cellular and Structural Biology and Barshop Institute on Longevity and Aging Studies, University of Texas Health Center at San Antonio, San Antonio, TX 78284, USA. [9]Department of Otolaryngology, University of Tokyo, Bunkyo-ku, Tokyo 113-8657, Japan.

*To whom correspondence should be addressed. E-mail: taprolla@wisc.edu

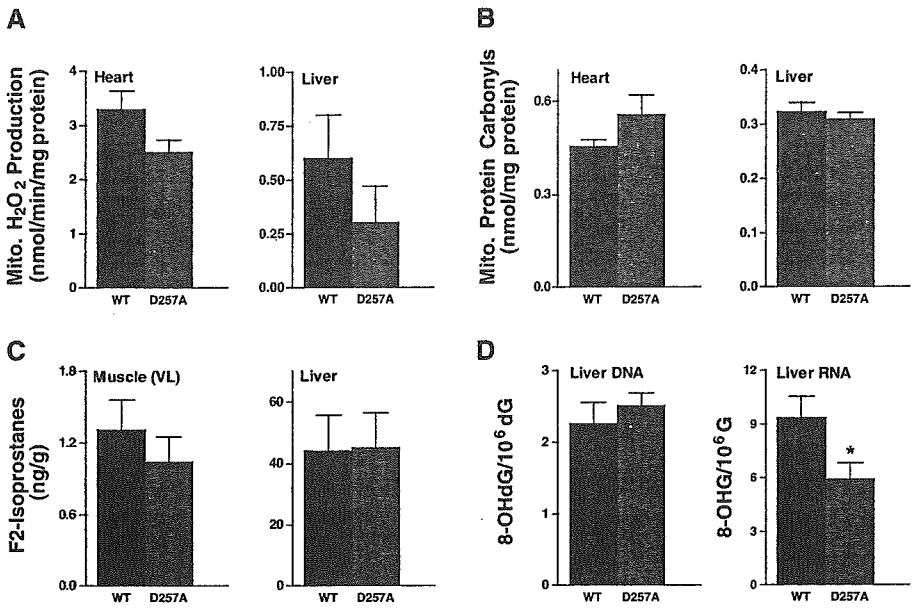

Fig. 2. Oxidative stress markers in isolated mitochondria and tissues from D257A mice. (**A**) Hydrogen peroxide production was measured by a sensitive fluorometric assay in mitochondria from wild-type (WT) and D257A mice at 9 months of age ($N \geq 8$). (**B**) Protein carbonyl levels, a marker of protein oxidation, were measured by an enzyme immunoassay in isolated mitochondria from WT and D257A mice at 9 months of age ($N \geq 7$). (**C**) F2-isoprostanes were measured by gas chromatography–negative ion chemical ionization mass spectrometry in liver and skeletal muscle (vastus lateralis) tissues from 6-month-old WT and D257A mice ($N = 6$). (**D**) Oxidative damage to DNA (8-OHdG) and RNA (8-OHG) was measured by high-performance liquid chromatography in liver tissue of 9-month-old WT and D257A mice ($N = 9$). *$P < 0.05$; error bars represent SEM.

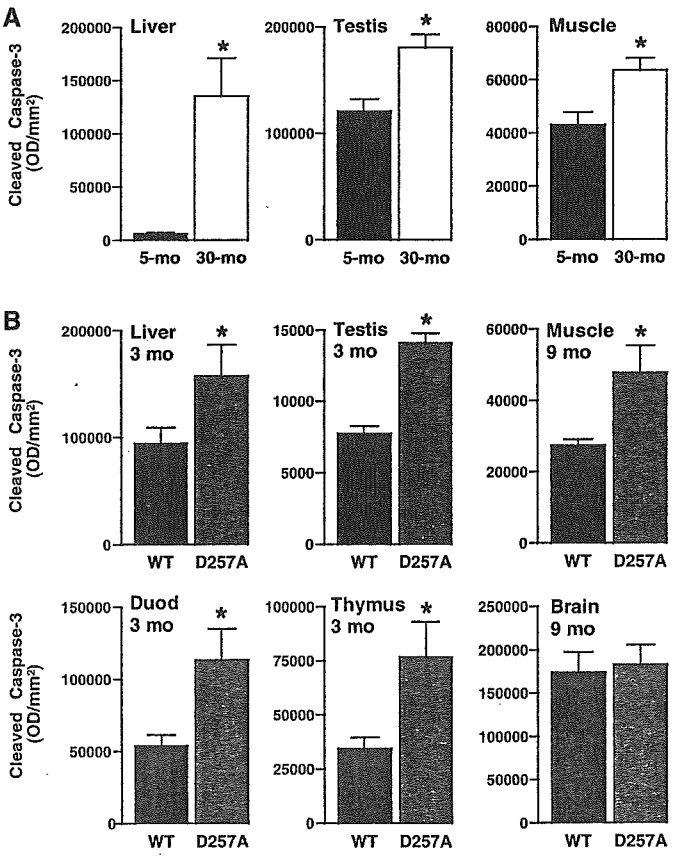

Fig. 3. Caspase activation in D257A mice and in normal aging. (**A**) Comparison of young (5 month) versus old (30 month) wild-type tissues. (**B**) Comparison of wild-type (WT) and D257A tissues at 3 months and 9 months of age. Activation of caspase-3 requires proteolytic processing of its inactive zymogen into activated fragments. The antibody used detects endogenous levels of the large fragment (17 to 19 kD) of activated caspase-3 resulting from cleavage adjacent to Asp^{175}. Extracts of tissues from WT and D257A mice of the indicated ages were subjected to SDS–polyacrylamide gel electrophoresis (PAGE) and probed with a rabbit monoclonal antibody to cleaved caspase-3 (5A1, Cell Signaling, Beverly, MA). Units are arbitrary OD units. For all tissues shown except brain, the difference between WT and D257A mice was significant ($N = 6$ to 8, *$P < 0.05$); error bars represent SEM. Duod, duodenum; Muscle, gastrocnemius.

D257A mice, maximum survival 460 days, median survival 416 days; for wild-type littermates, maximum and median survival >850 days; $P < 0.0001$; Fig. 1C) and displayed several overt phenotypes in tissues undergoing rapid cellular turnover. These phenotypes were age-related and included thymic involution, testicular atrophy associated with the depletion of spermatogonia, loss of bone mass, loss of intestinal crypts, progressive decrease in circulating red blood cells, and weight loss (figs. S2 to S4).

Age-related hearing loss (presbycusis) is a hallmark of aging in multiple species, including mice (*10*) and humans (*11*), and has been correlated with the age-related accumulation of mtDNA mutations in auditory tissue. Hearing loss can be monitored by an elevation in auditory-evoked brainstem response (ABR). We conducted ABR analysis and observed no difference in auditory function between wild-type and D257A mice at 2 months of age (fig. S5G), but we found marked elevation of ABR thresholds at 4, 8, and 16 kHz ($P < 0.0001$) in D257A mice by 9 months of age, indicating severe hearing loss (fig. S5H). Histological analysis revealed age-related loss of spiral ganglion neurons (fig. S5), a feature of presbycusis (*12*). Thus, accumulation of mtDNA mutations can have a causal role in presbycusis.

Aging in rodents (*13*) and humans (*14*) is also characterized by loss of muscle mass (sarcopenia). Consistent with a causal role for mtDNA mutations in sarcopenia, the D257A mice displayed age-related loss of skeletal muscle. At 3 months of age, muscle weight in the D257A mice was similar to that of wild-type mice (fig. S6A); at 9 months of age, however, the mutant mice showed a significant reduction in the weight of both gastrocnemius ($P < 0.002$, ~10% decrease) and quadriceps ($P < 0.005$, ~10% decrease) muscles (fig. S6B). Therefore, age-related accumulation of mtDNA mutations is likely to contribute to sarcopenia.

To determine whether mtDNA mutations accumulated to varying extents in different tissues of the D257A mice, we sequenced a 525–base pair (bp) region of mtDNA that spans the control region, as well as a 487-bp region of the *COX1* gene. Sequencing revealed that the frequency of mtDNA mutations in the mutant mice was ~3 to 8 times that in wild-type mice for most tissues examined (fig. S7). Surprisingly, the frequency of mtDNA mutations in 5-month-old wild-type mice was as high as 2.1×10^{-4} in the *COX1* gene and 5.9×10^{-4} in the control region. This corresponds to average mutation frequencies of ~4 and ~10 mutations per mitochondrial genome, respectively.

A fraction of the oxygen consumed by cells results in the production of superoxide ($O_2^{\bullet-}$) in mitochondria, which is dismutated to hydrogen peroxide (H_2O_2) by superoxide dismutase. The main tenet of the free radical theory

of aging (*15*) is that aging is due to the progressive accrual of ROS-inflicted damage, including mtDNA mutations, the accumulation of which has been postulated to lead to a "vicious cycle" of further mitochondrial ROS generation and mitochondrial dysfunction (*1*, *2*). To test this hypothesis, we measured H_2O_2 produced by mitochondria isolated from the heart and liver of young and old (3 months versus 9 months) D257A and wild-type mice. Levels of H_2O_2 were not significantly different between genotypes in either young or old heart or liver mitochondria (Fig. 2A) (fig. S8A). We also assayed protein carbonyls, a marker of oxidative damage to proteins, and found no significant differences between 9-month-old D257A and wild-type mice in mitochondrial (Fig. 2B) or cytosolic fractions (fig. S8B) of either heart or liver. Thus, despite increased mutational load, mitochondria from D257A mice do not show increased oxidative stress.

We next examined additional markers of ROS-induced damage in tissues of D257A and wild-type mice. We measured F2-isoprostanes, a marker of lipid peroxidation (*16*), in liver, skeletal muscle (Fig. 2C), and heart (fig. S8C), and observed no significant differences between 6-month-old D257A mice and wild-type controls. We also examined oxidative damage to RNA and DNA in 9-month-old D257A and wild-type mice. Liver DNA from wild-type and mutant mice had similar levels of 8-hydroxy-2′-deoxyguanosine (8-OHdG) (Fig. 2D). Interestingly, liver RNA from the D257A mice had lower steady-state levels of 8-hydroxyguanosine (8-OHG) relative to samples from wild-type mice (Fig. 2D, $P < 0.05$). Thus, our observations do not support the idea that mtDNA mutations contribute to increased ROS production and oxidative stress in mitochondria with age.

One possible mechanism for the phenotypes in mitotic tissues of D257A mice is a defect in cellular proliferation. We derived mouse embryonic fibroblast lines (MEFs) from D257A and wild-type littermates and measured the number of cell doublings before senescence. At 20% oxygen, both wild-type and D257A MEFs underwent rapid replicative senescence, whereas neither underwent senescence or reduced growth after 40 days of culture at 2% oxygen (fig. S9). Thus, accelerated aging in D257A mice is not likely to be due to an intrinsic defect in cellular proliferation, or to accelerated cellular senescence.

In the mitochondrial pathway of apoptosis, mitochondrial dysfunction can lead to mitochondrial outer membrane permeabilization, the release of cytochrome c into the cytosol, and the activation of a key effector protease, caspase-3, by proteolytic cleavage (*17*, *18*). To determine whether an increased level of cleaved caspase-3 is a feature of normal aging, we examined tissues of 5-month-old and 30-month-old wild-type mice by immunoblotting. Cleaved caspase-3 levels increased with aging in liver, skeletal muscle, testis (Fig. 3A), and heart (fig. S10A) of wild-type mice by ~50% or greater. We also monitored the extent of apoptosis in tissues of D257A and wild-type mice. Levels of cleaved caspase-3 were significantly elevated in the cytosolic fractions of duodenum, liver, testis, and thymus of 3-month-old D257A mice relative to wild-type controls (Fig. 3B), and this induction preceded phenotypes in most tissues. Levels of cleaved caspase-3 were not altered in 3-month-old D257A skeletal muscle and brain relative to wild-type samples (fig. S10B), which suggests that postmitotic tissues may be more resistant to the induction of apoptosis mediated by mtDNA mutations. Cleaved caspase-3 levels were increased, however, in D257A skeletal muscle at 9 months of age relative to controls (Fig. 3B), a time at which mutant animals displayed loss of muscle mass. Thus, normal aging is associated with the activation of a caspase-3–mediated apoptotic pathway in several tissues, and D257A mice display an early onset of this phenotype.

Apoptosis is also associated with nuclear DNA fragmentation. Because the intestinal epithelium, thymus, and testis were severely affected in D257A mice, we examined these tissues with the TUNEL (terminal deoxynucleotidyl transferase–mediated deoxyuridine triphosphate nick end labeling) assay, which detects apoptotic cells in situ. The 3-month-old D257A mice showed significantly more TUNEL positive cells relative to wild-type mice in all tissues examined (Fig. 4). Together, these findings strongly suggest that loss of critical, irreplaceable cells through apoptosis is a central mechanism of tissue dysfunction associated with the accumulation of mtDNA mutations.

We have demonstrated that accelerated development of aging phenotypes through mtDNA mutations can occur in the absence of increased ROS production or oxidative stress, and that tissue dysfunction is likely to arise through increased apoptosis. Moreover, we have shown that increased caspase-3 activation occurs in multiple tissues with normal aging. Tissues that are composed of mitotic cells display early caspase-3 activation in D257A mice, whereas skeletal muscle displays a later increase in cleaved caspase-3 and associated tissue degeneration. It is also clear that some cell types, such as spiral ganglion neurons, are exquisitely sensitive to the effects of age-related accumulation of mtDNA mutations. Because D257A mice display high levels of mtDNA mutations, it is possible that some of the phenotypes in these animals may be due to

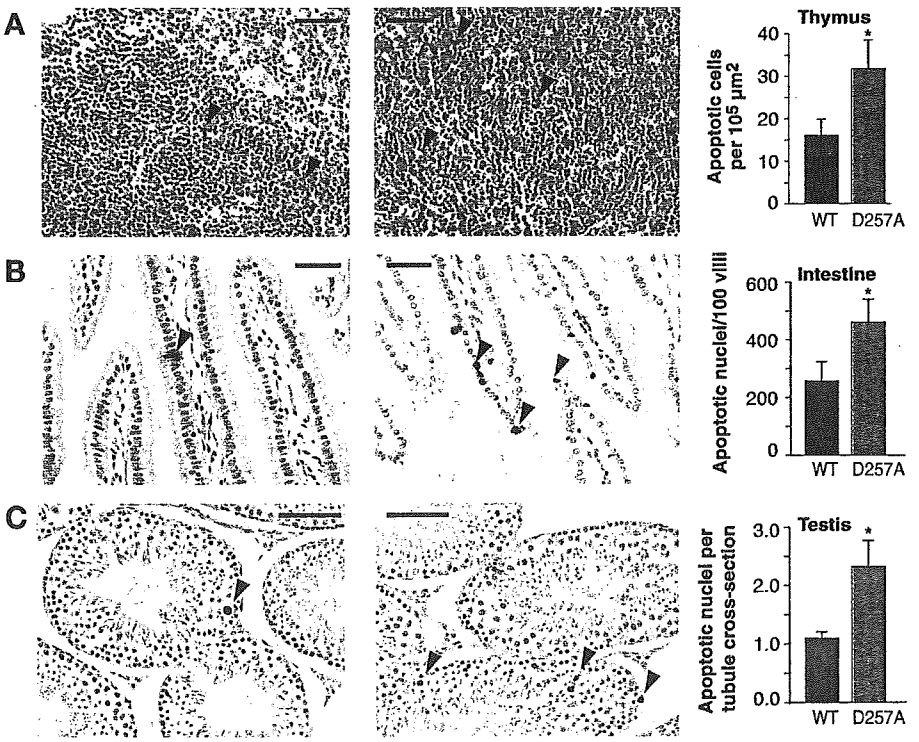

Fig. 4. Quantification of apoptosis by TUNEL in thymus (A), small intestine (B), and testis (C) of 3-month-old WT (left panels) and D257A (center panels) mice. Arrowheads indicate TUNEL-positive apoptotic nuclei. Numbers of apoptotic nuclei per 10^5 µm² section (thymus), per 100 villi (intestine), and per seminiferous tubule cross section (testis) were counted in hematoxylin-counterstained sections from the indicated genotypes. Each bar represents apoptotic nuclei from intestinal, thymus, and testis sections of at least four mice per genotype. *$P < 0.05$; error bars represent SEM. Scale bar, 100 µm.

complete exhaustion of tissue regenerative capacity, a process that may not be as severe in normal aging. However, the wide tissue distribution of phenotypes in D257A mice suggests that the age-related accumulation of mtDNA mutations reported in several species (*3*–*7*) contributes to physiological decline.

The concept that DNA damage contributes to aging is supported by the finding that humans and mice carrying mutations in several genes involved in DNA repair, including *Ercc2* (*Xpd*) (*19*), *Xrcc5* (*Ku86*) (*20*), and *Wrn* (*21*), display premature aging syndromes. It is likely that several types of DNA damage contribute to the aging process, and our findings suggest that apoptosis and subsequent loss of irreplaceable cells may be an important mechanism of aging in mammals. In agreement with this hypothesis, caloric restriction, the only nutritional intervention that retards aging, delays the accumulation of mtDNA mutations (*22*) and reduces mitochondria-mediated apoptotic pathways (*23*, *24*).

References and Notes

1. D. Harman, *J. Am. Geriatr. Soc.* **20**, 145 (1972).
2. J. E. Fleming, J. Miquel, S. F. Cottrell, L. S. Yengoyan, A. C. Economos, *Gerontology* **28**, 44 (1982).
3. Y. Wang *et al.*, *Proc. Natl. Acad. Sci. U.S.A.* **98**, 4022 (2001).
4. S. Melov, D. Hinerfeld, L. Esposito, D. C. Wallace, *Nucleic Acids Res.* **25**, 974 (1997).
5. M. Corral-Debrinski *et al.*, *Nat. Genet.* **2**, 324 (1992).
6. C. M. Lee, S. S. Chung, J. M. Kaczkowski, R. Weindruch, J. M. Aiken, *J. Gerontol.* **48**, B201 (1993).
7. M. Khaidakov, R. H. Heflich, M. G. Manjanatha, M. B. Myers, A. Aidoo, *Mutat. Res.* **526**, 1 (2003).
8. A. Trifunovic *et al.*, *Nature* **429**, 417 (2004).
9. See supporting data on *Science* Online.
10. Q. Y. Zheng, K. R. Johnson, L. C. Erway, *Hear. Res.* **130**, 94 (1999).
11. M. A. Gratton, A. E. Vazquez, *Curr. Opin. Otolaryngol. Head Neck Surg.* **11**, 367 (2003).
12. E. M. Keithley, C. Canto, Q. Y. Zheng, N. Fischel-Ghodsian, K. R. Johnson, *Hear. Res.* **188**, 21 (2004).
13. J. Wanagat, Z. Cao, P. Pathare, J. M. Aiken, *FASEB J.* **15**, 322 (2001).
14. J. Lexell, C. C. Taylor, M. Sjostrom, *J. Neurol. Sci.* **84**, 275 (1988).
15. D. Harman, *J. Gerontol.* **11**, 298 (1956).
16. L. J. Roberts 2nd, J. D. Morrow, *Cell. Mol. Life Sci.* **59**, 808 (2002).
17. D. R. Green, G. Kroemer, *Science* **305**, 626 (2004).
18. M. O. Hengartner, *Nature* **407**, 770 (2000).
19. J. de Boer *et al.*, *Science* **296**, 1276 (2002).
20. H. Vogel, D. S. Lim, G. Karsenty, M. Finegold, P. Hasty, *Proc. Natl. Acad. Sci. U.S.A.* **96**, 10770 (1999).
21. S. Chang *et al.*, *Nat. Genet.* **36**, 877 (2004).
22. L. E. Aspnes *et al.*, *FASEB J.* **11**, 573 (1997).
23. R. R. Shelke, C. Leeuwenburgh, *FASEB J.* **17**, 494 (2003).
24. H. Y. Cohen *et al.*, *Science* **305**, 390 (2004).

25. We thank J. Warren for stem cell injections, S. Kinoshita for histological processing, and D. Carlson for support in mouse colony management. Supported by NIH grants AG021905 (T.A.P.), AG18922 (R.W.), AG17994 (C.L.), AG21042 (C.L.), DK48831, GM15431, and RR00095 (J.D.M.), and AG16694 (J.M.S.); by NIH training grants T32 AG00213 (G.C.K.) and T32 GM07601 (W.A.J.); and by American Heart Association predoctoral fellowship 0415166B (A.H.). R.W. and T.A.P. are founders and members of the board of LifeGen Technologies, a company focused on nutritional genomics, including the impact of nutrients and caloric restriction on the aging process.

Supporting Online Material

www.sciencemag.org/cgi/content/full/309/5733/481/DC1
Materials and Methods
Figs. S1 to S10

11 March 2005; accepted 25 May 2005
10.1126/science.1112125

Available online at www.sciencedirect.com
SCIENCE DIRECT®
Neuroscience Letters 395 (2006) 18–22
Neuroscience Letters
www.elsevier.com/locate/neulet

Cochlear damage due to germanium-induced mitochondrial dysfunction in guinea pigs

Tatsuya Yamasoba [a,*], Yu-ichi Goto [b], Hirofumi Komaki [b], Masakazu Mimaki [b], Akira Sudo [b], Mitsuya Suzuki [a]

[a] *Department of Otolaryngology, Head and Neck Surgery, University of Tokyo, Hongo 7-3-1, Bunkyo-ku, Tokyo 113-8655, Japan*
[b] *Department of Mental Retardation and Birth Defect Research, National Institute of Neuroscience, National Center of Neurology and Psychiatry, Tokyo, Japan*

Received 24 August 2005; received in revised form 17 October 2005; accepted 17 October 2005

Abstract

This investigation addressed the effect of germanium dioxide (GeO_2)-induced mitochondrial dysfunction on hearing acuity. Guinea pigs were fed chow that contained 0%, 0.15%, or 0.5% GeO_2. The animals that were fed 0.5% GeO_2 for 2 months developed hearing impairment chiefly due to degeneration of stria vascularis and cochlear supporting cells, which exhibited electron-dense mitochondrial inclusions. Cytochrome *c* oxidase activity was decreased in the skeletal muscles and kidney, which also exhibited electron-dense mitochondrial inclusions. No apparent pathological changes were observed in the utricle, semicircular canal, or among the vestibular nerve fibers, or in the liver or heart. The untreated animals and those treated with 0.15% GeO_2 did not exhibit hearing impairment or pathological changes in any organs. These findings suggest that administration of 0.5% GeO_2 induces mitochondrial dysfunction in the stria vascularis and supporting cells in the cochlea, as in the skeletal muscles and kidney, thereby causing hearing impairment in the guinea pigs.

Keywords: Hearing loss; Mitochondrial myopathy; Mitochondrial DNA; Cochlea; Muscle; Kidney

Mutations in mitochondrial DNA (mtDNA) are reported to be closely associated with both syndromic and nonsyndromic forms of sensorineural hearing loss (SNHL) [14]. SNHL occurs in approximately 70% of the three most common mitochondrial disorders: mitochondrial myopathy, encephalopathy, lactic acidosis and stroke-like episodes (MELAS), myoclonus epilepsy associated with ragged-red fiber, and chronic progressive external ophthalmoplegia (CPEO) [14]. SNHL is also frequently manifested in subjects with other mtDNA mutations, particularly those in 12S rRNA and $tRNA^{Ser(UCN)}$ [2]. In general, SNHL due to mtDNA lesions primarily involves the cochlea, while the vestibular system and retrocochlear auditory pathway are well preserved [1,11,17]. The fact that mtDNA lesions frequently cause SNHL of cochlear origin suggests that certain sets of cochlear cells have a high metabolic demand and are strongly dependent upon mitochondrial function. Human temporal bone histopathology has been reported only in four patients with SNHL associated with mtDNA lesions [7,13,20], in which the stria vascularis (SV) exhibited degeneration but other cochlear tissues such as hair cells were not always affected. It is therefore unclear which cochlear cells are preferentially affected by chronic mitochondrial dysfunction associated with mtDNA lesions.

There are several animal models, including genetically modified mice, that exhibit certain forms of mitochondrial dysfunction [15]. Auditory function has been studied in mice with mutant mtDNA carrying a 4696-base pair deletion, which develop hearing loss when the heteroplasmy is greater than 80% [8]. To date, cochlear histopathology has not been studied in these mice. Other animal models can be created by introducing harmful agents into the mitochondria. Hoya et al. [5] applied a mitochondrial toxin, 3-nitropropionic acid (3-NP), topically to rat cochlea and found that animals treated with 500 mM of 3-NP exhibited permanent threshold shifts. Histologically, there was degeneration of fibrocytes in the spiral ligament and spiral limbus, which indicated that these tissues may be vulnerable to acute mitochondrial dysfunction. Another animal model was created by chronic application of germanium

* Corresponding author. Tel.: +81 3 5800 8924; fax: +81 3 3814 9486.
E-mail address: tyamasoba-tky@umin.ac.jp (T. Yamasoba).

0304-3940/$ – see front matter © 2005 Elsevier Ireland Ltd. All rights reserved.
doi:10.1016/j.neulet.2005.10.045

dioxide (GeO_2). This model is of special interest since in humans, long-term administration of high doses of GeO_2 causes renal failure, emaciation, and muscle weakness [3,10]. Germanium compounds are readily absorbed following oral exposure, distributed throughout the body tissues, particularly the kidney and thyroid, and excreted largely in the urine. Rats that are fed chow containing GeO_2 exhibit body weight loss, myopathy, and nephropathy, and their skeletal muscles show numerous ragged-red fibers, cytochrome *c* oxidase (COX)-deficient fibers, and accumulation of electron-dense material in the mitochondria [3,4,9,16]. These pathological findings resemble those observed in patients with mitochondrial encephalomyopathy. Although the precise mechanism of toxicity of GeO_2 is unknown, recent study demonstrated that rats treated with GeO_2 for 24 weeks' showed increased free radical generation and decreased mitochondrial DNA copies in the skeletal muscles compared to controls given normal diet [6]. Thus, chronic administration of GeO_2 may provide a controlled model for assessment of mitochondrial dysfunction-induced SNHL and allow analysis of the specific histopathology underlying this clinically significant disorder.

Thirty-six albino male guinea pigs (250–300 g, approximately 4 weeks after birth) with auditory brainstem response (ABR) thresholds within the normal laboratory range were used. Twelve animals were assigned to one of the three groups and fed standard guinea pig chow containing 0% (control), 0.15%, or 0.5% GeO_2. The controls and animals that were administered 0.15% GeO_2 were allowed to survive for 6 months, but animals administered 0.5% GeO_2 were sacrificed after 2 months because many became inactive and appeared less healthy at that time. Animals were caged singularly in an ambient room under a 12-h light:12-h dark cycle beginning at 06:00 h. Food and water were available ad libitum. Clinical manifestations and the body weight of each animal were observed every 2 weeks. Pure-tone ABRs were measured every 4 weeks. The experimental protocol was approved by the Committee for the Use and Care of Animals at the University of Tokyo and conformed to the NIH Guidelines for the Care and Use of Laboratory Animals.

The method for ABR measurement has been previously described [19]. In brief, the animals were anesthetized with xylazine hydrochloride (10 mg/kg, i.m.) and ketamine hydrochloride (40 mg/kg, i.m.). Following anesthetization, needle electrodes were placed subcutaneously at the vertex (active electrode), beneath the pinna of the left ear (reference electrode), and beneath the right ear (ground). The sound stimulus consisted of a 15-ms tone burst, with a rise-fall time of 1 ms at frequencies of 2, 4, 8, and 16 kHz. The responses of 1024 sweeps were averaged at each intensity level (5 dB steps) to assess the threshold. Hearing threshold was defined as the lowest stimulus intensity that produced a reliable peak 3 or 4 in ABR waveforms. The effect of GeO_2 on the ABR thresholds was analyzed by comparing the final thresholds, measured 2 month later for animals that were administered 0.5% GeO_2 and 6 month later for those given 0.15% GeO_2 and controls, among the three groups using one-way ANOVA followed by a multiple comparison procedure (Student–Newman–Keuls method).

The controls and animals that were administered 0.15% GeO_2 were sacrificed 6 months later. The animals that were administered 0.5% GeO_2 were sacrificed after 2 months because most of them became very inactive and seemingly unhealthy at that time. Under anesthesia with xylazine hydrochloride (10 mg/kg, i.m.) and ketamine hydrochloride (40 mg/kg, i.m.), the bulla in the left ear was exposed, a small opening was made in the scala tympani, and the perilymphatic spaces were perfused with a fixative containing 2% paraformaldehyde and 2.5% glutaraldehyde in phosphate buffer. This was followed by immediate excision of the soleus and extensor digitorum longus (EDL) muscles, liver, kidney, and heart. A part of these organs was quickly frozen in isopentane chilled in liquid nitrogen, and the remaining specimens were immersed in the fixative. The left temporal bone was then excised, immersed in the same fixative, decalcified in 10% ethylenediaminetetraacetic acid, and divided into cochlear and vestibular parts. The cochlea was incised parallel to the modiolus and the utricular macula and ampulla of the lateral semicircular canal were obtained. For electron microscopy, all the fixed specimens (muscle, liver, kidney, heart, cochlea, utricle, and lateral semicircular canal) were post-fixed in 1% osmium tetroxide, dehydrated in a graded ethanol series, and embedded in epoxy resin. Ultrathin sections were double stained with uranyl acetate and lead citrate and examined with a transmission electron microscope (TEM), as previously described [18]. Serial frozen sections of the skeletal muscle, heart, kidney, and liver were also stained with hematoxylin and eosin (H&E) and an antibody to COX, as previously described [16].

In the controls and animals that were administered 0.15% GeO_2, the body weight increased gradually from 280 to 780 g during a period of 6 months. In contrast to this, the weight of animals that were administered 0.5% GeO_2 increased slightly to 310 g in the first month and reduced to 295 g in the second month (Fig. 1). The weight loss was accompanied by muscle weakness and atrophy, but none of the animals exhibited apparent neurological abnormalities such as ataxia or convulsions.

The controls and animals that were administered 0.15% GeO_2 did not demonstrate shifts in the ABR threshold compared with their baseline values at any frequency during the experiment, whereas the animals that were administered 0.5% GeO_2 exhibited significant increase ($p < 0.01$) in the ABR thresholds at all frequencies 2 months later (Fig. 1).

The most prominent findings in the animals that were administered 0.5% GeO_2 were marked degeneration of the SV and supporting cells in the organ of Corti (Fig. 2). Vacuolar degeneration, accompanied by abnormal mitochondria containing electron-dense inclusions, was predominantly observed in the SV of the basal turns of the cochlea. Electron-dense mitochondrial inclusions were also observed in the Hensen cells, Boettcher cells, and Claudius cells, all of which showed marked degenerative changes. The inner and outer hair cells (IHCs and OHCs, respectively), pillar cells, and Deiters cells, as well as the basilar and tectorial membranes, showed no obvious signs of pathology. A small amount of electron-dense material was observed along the intact cochlear nerve fibers. No electron-dense material or pathological changes were observed in the utricle, lateral semicircular canal, or among the vestibular nerve

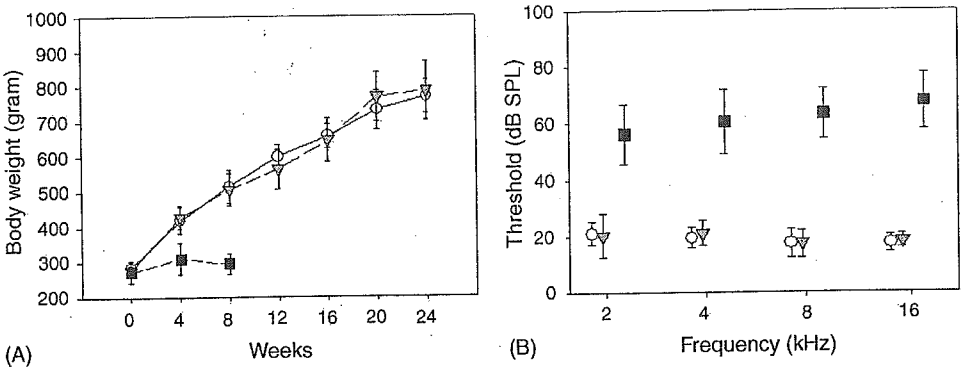

Fig. 1. (A) Change (mean ± S.D.) in whole body weight. (B) Auditory brainstem response thresholds (mean ± S.D.) measured before euthanasia, i.e., 6 months after the initiation of the experiment in controls (○) and animals that were administered 0.15% GeO_2 (▽) and 2 months after the initiation in those that were administered 0.5% GeO_2 (■).

fibers. In the controls and animals that were administered 0.15% GeO_2, no pathological changes or electron-dense material were observed in the cochlea or vestibular endorgans or among the cochlear or vestibular nerve fibers (data not shown).

In the animals that were administered 0.5% GeO_2, marked pathological and histochemical changes were observed in the skeletal muscles and kidney. The EDL and soleus muscles, which contained many abnormal mitochondria including electron-dense material, showed marked reduction in COX activity when compared with that of the controls (Fig. 3). Similarly, the kidney exhibited vacuolar degeneration and many electron-dense deposits in the distal tubular epithelium and reduction in COX activity. No apparent morphological or histochemical abnormalities were found in the liver or heart, although a small amount of electron-dense inclusions were observed in the mitochondria of the heart. The controls and animals that were administered 0.15% GeO_2 did not show any evidence of pathological changes in any tissue examined. COX activity did not differ in any organs between these groups (data not shown).

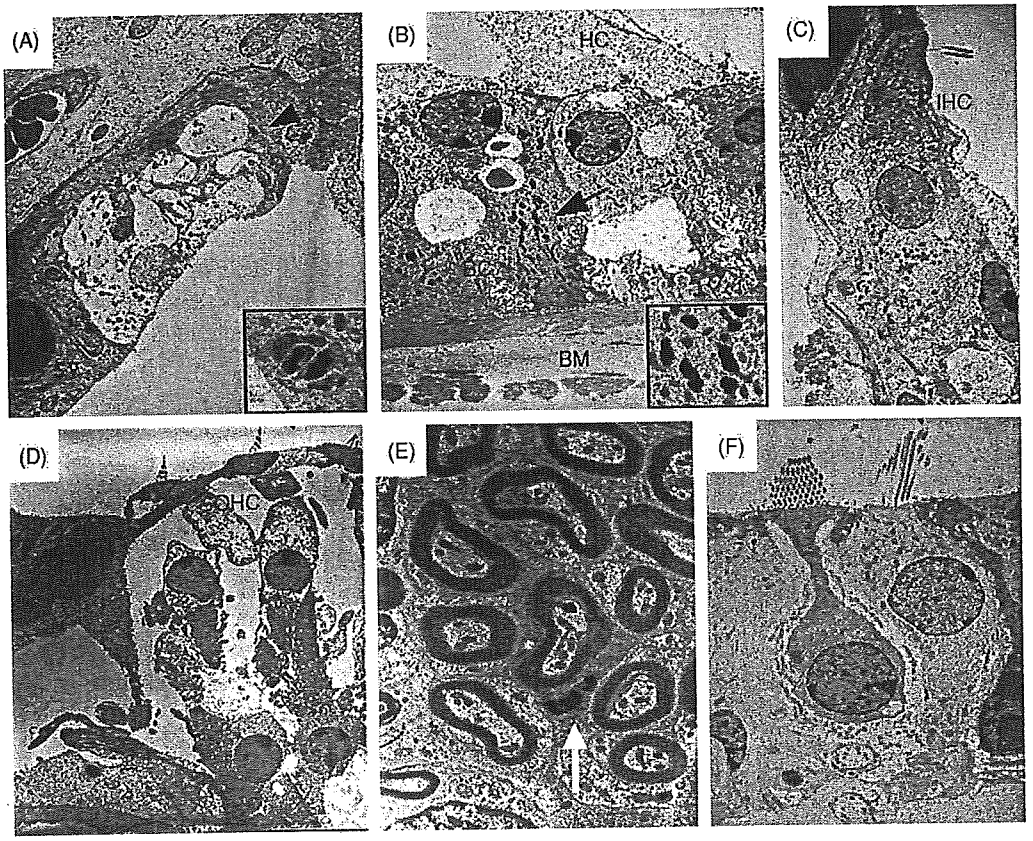

Fig. 2. Ultrastructural findings of the inner ear in animals that were administered 0.5% GeO_2. (A) Marked vacuolar degeneration in the stria vascularis (SV). The arrowhead indicates mitochondria containing electron-dense inclusions (inset: high-power view). (B) The supporting cells, such as Hensen cells (HC) and Boettcher cells (BC), in the organ of Corti show marked degenerative changes. The arrowhead indicates the mitochondria containing electron-dense materials (inset: high-power view); BM: basilar membrane. (C) Relatively well preserved inner hair cell (IHC). (D) Relatively well preserved outer hair cells (OHC) and pillar cells (PC). (E) A small amount of mitochondria containing electron-dense materials (white arrow) along the intact cochlear nerve fibers. (F) Normal sensory epithelium of the utricle.

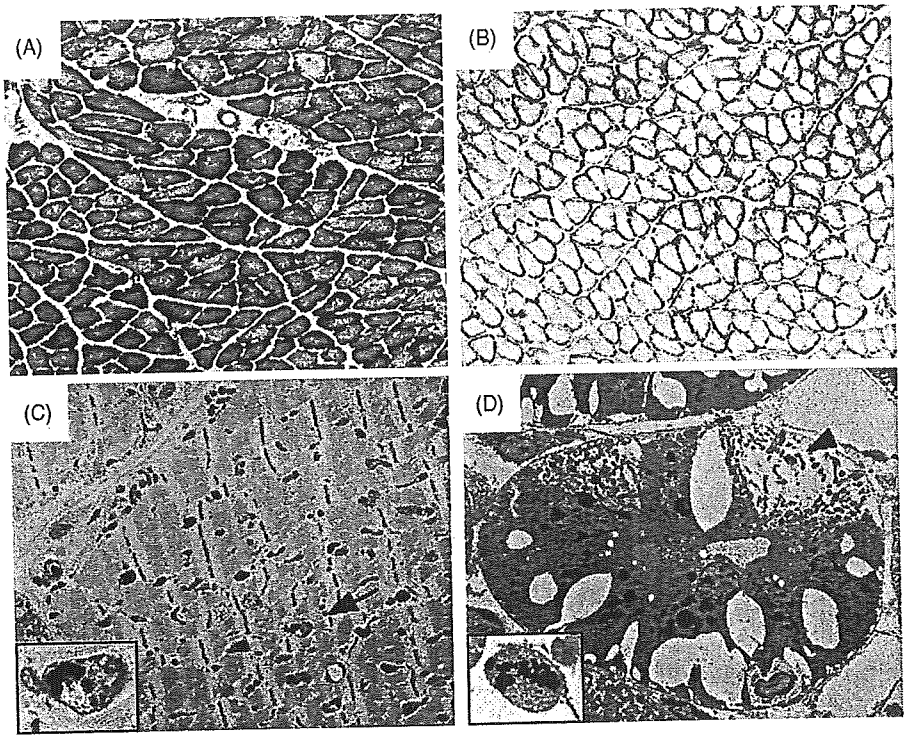

Fig. 3. Frozen sections of the soleus muscle stained with COX from a control (A) and an animal that was administered 0.5% GeO_2 (B), showing marked reduction in COX activity in the latter. Ultrastructural findings in extensor digitorum longus muscle (C) and kidney (D) from an animal that was administered 0.5% GeO_2. The arrow indicates the muscle showing many degenerated mitochondria containing electron-dense materials (inset: high-power view). The arrowhead indicates the distal tubular epithelium in kidney showing vacuolar degeneration and many electron-dense deposits (inset: high-power view).

The current study showed that chronic administration of 0.5% GeO_2, and not 0.15% GeO_2, in guinea pigs caused degeneration of the skeletal muscles and kidney, which was associated with electron-dense materials in the mitochondria and the reduction in COX activity. The animals that were administered 0.5% GeO_2 also developed severe hearing loss chiefly due to the degeneration of SV and cochlear supporting cells, both of which contained a large amount of electron-dense materials in the mitochondria. These findings suggest that SV and the supporting cells in the cochlea are most preferentially affected by chronic mitochondrial dysfunction in guinea pigs.

While the controls and animals that were administered 0.15% GeO_2 showed gradual increase in the body weight from 280 to 780 g during a period of 6 months, the weight of animals that were administered 0.5% GeO_2 increased only slightly in the first month and reduced in the second month, which is considered to primarily reflect the loss of muscle mass due to GeO_2-induced mitochondrial damage. It is also possible that animals that were administered 0.5% GeO_2 ate less than those in the other groups, and may not have consumed on the average 3 1/3 times the amount of GeO_2 consumed by the animals administered 0.15% GeO_2 in that same period.

The pathological changes in the skeletal muscles and kidney of guinea pigs that were administered 0.5% GeO_2 were very similar to those observed in rats that were administered 0.15% GeO_2 and human subjects who were administered high doses of GeO_2 for a long period of time [3,4,9,10,16]. In a preliminary study, we found that mice that were administered 0.15% GeO_2 also developed body weight loss, degeneration of the skeletal muscles and kidney containing electron-dense materials in the mitochondria, and severe hearing loss (Yamada et al., unpublished data). These findings suggest that chronic mitochondrial dysfunction unexceptionally causes the above-mentioned pathologies in mammals, although the GeO_2 concentration that causes mitochondrial dysfunction may differ among species.

Human temporal bone histopathological findings associated with mtDNA lesions have been reported in four patients. In a patient with MELAS and moderate SNHL, marked SV atrophy, partial loss of the IHCs and OHCs, moderate loss of the spiral ganglion cells (SGCs), and loss of sensory cells in the vestibular endorgans were observed [13]. Another patient with MELAS and moderate SNHL exhibited severe SV atrophy, intact IHCs and OHCs, and only mildly degenerated SGCs [13]. A totally deaf patient with Kearns–Sayre syndrome, a form of CPEO, exhibited marked degeneration of the SV, spiral prominence, and organ of Corti; slight reduction in the number of SGCs; and well preserved semicircular canals and utricle [7]. A totally deaf patient with maternally inherited diabetes and deafness associated with A3243G mutation exhibited marked SV atrophy, partial loss of the OHCs, and loss of the SGCs in the basal turn, whereas the IHCs and vestibular endorgans were well preserved [20]. These findings suggest that in humans, SV is the first to be affected by mitochondrial dysfunction; the organ of Corti including the supporting cells, the second; the SGCs, the third; and vestibular endorgans, the last. This pattern of inner ear cell involvement in human mtDNA lesions is similar to that observed in the guinea pigs that were administered 0.5% GeO_2, which is indicative of the fact that animals treated with GeO_2

can be used to study the mechanism of hearing impairment and cochlear damage associated with mtDNA lesions.

Many previous animal studies that investigated noise-induced or aminoglycoside-induced damage have shown that the OHCs are more vulnerable to these stresses compared to the IHCs and supporting cells [12,19]. In contrast, in the current study, the supporting cells were damaged while the IHCs and OHCs remained nearly intact. GeO_2 may have been distributed more preferentially to the supporting cells, resulting in their preferential degeneration. Alternatively, the supporting cells may be more susceptible to mitochondrial dysfunction than the hair cells. In either case, the histological findings suggest that we need to check more carefully the status of supporting cells of the organ of Corti in studies of stress induced damage.

In conclusion, the current study suggests that chronic mitochondrial dysfunction may most preferentially affect the SV and supporting cells in the guinea pig cochlea. This animal model is considered useful for studying the SNHL mechanism associated with mtDNA lesions. The next step is to determine the genes that are involved in SNHL development in this animal model, which provides invaluable information on the prevention/retardation of SNHL in patients harboring mtDNA lesions. It may also be worthwhile to examine if the manifestation of phenotype in this animal model can be prevented or retarded by calorie restriction, which causes a metabolic shift toward increased protein turnover and decreased macromolecular damage, and by supplements, such as alpha lipoic acid and acetyl-L-carnitine, that have a capacity to enhance mitochondrial bioenergetics.

Acknowledgments

This work was supported by grants from the Ministry of Health, Labour and Welfare and the Ministry of Education, Culture, Sports, Science and Technology in Japan to Tatsuya Yamasoba. We thank Mr. Y. Mori for providing us with technical assistance.

References

[1] P.F. Chinnery, C. Elliot, G.R. Green, A. Rees, A. Coulthard, D.M. Turnbull, T.D. Griffiths, The spectrum of hearing loss due to mitochondrial DNA defects, Brain 123 (2000) 82–92.
[2] N. Fischel-Ghodsian, Mitochondrial deafness, Ear Hear 24 (2003) 303–313.
[3] I. Higuchi, S. Izumo, M. Kuriyama, M. Suehara, M. Nakagawa, H. Fukunaga, M. Osame, S. Ohtsubo, K. Miyata, Germanium myopathy: clinical and experimental pathological studies, Acta Neuropathol. (Berl.) 79 (1989) 300–304.
[4] I. Higuchi, K. Takahashi, K. Nakahara, E. Izumo, M. Nakagawa, M. Osame, Experimental germanium myopathy, Acta Neuropathol. (Berl.) 82 (1991) 55–59.
[5] N. Hoya, Y. Okamoto, K. Kamiya, M. Fujii, T. Matsunaga, A novel animal model of acute cochlear mitochondrial dysfunction, NeuroReport 15 (2004) 1597–1600.
[6] X. Li, F. Gao, Q. Chen, The pathogenesis of experimental model of mitochondrial myopathy induced by germanium dioxide, Chin. Med. Sci. J. 16 (2001) 157–160.
[7] J.R. Lindsay, R. Hinojosa, Histopathologic features of the inner ear associated with Kearns–Sayre syndrome, Arch. Otolaryngol. 102 (1976) 747–752.
[8] K. Nakada, A. Sato, H. Sone, A. Kasahara, K. Ikeda, Y. Kagawa, H. Yonekawa, J. Hayashi, Accumulation of pathogenic DeltamtDNA induced deafness but not diabetic phenotypes in mito-mice, Biochem. Biophys. Res. Commun. 323 (2004) 175–184.
[9] T. Sanai, N. Oochi, S. Okuda, S. Osato, S. Kiyama, T. Komota, K. Iseki, M. Fujishima, Subacute nephrotoxicity of germanium dioxide in the experimental animal, Toxicol. Appl. Pharmacol. 103 (1990) 345–353.
[10] T. Sanai, S. Okuda, K. Onoyama, N. Oochi, Y. Oh, K. Kobayashi, K. Shimamatsu, S. Fujii, M. Fukushima, Germanium dioxide-induced nephropathy: a new type of renal disease, Nephron 54 (1990) 53–60.
[11] C.M. Sue, L.J. Lipsett, D.S. Crimmins, C.S. Tsang, S.C. Boyages, C.M. Presgrave, W.P. Gibson, E. Byrne, J.G. Morris, Cochlear origin of hearing loss in MELAS syndrome, Ann. Neurol. 43 (1998) 350–359.
[12] M. Sugawara, G. Corfas, M.C. Liberman, Influence of supporting cells on neuronal degeneration after hair cell loss, J. Assoc. Res. Otolaryngol. 6 (2005) 136–147.
[13] K. Takahashi, S.N. Merchant, T. Miyazawa, T. Yamaguchi, M.J. McKenna, H. Kouda, Y. Iino, T. Someya, Y. Tamagawa, Y. Takiyama, I. Nakano, K. Saito, P. Boyer, K. Kitamura, Temporal bone histopathological and quantitative analysis of mitochondrial DNA in MELAS, Laryngoscope 113 (2003) 1362–1368.
[14] D.C. Wallace, Diseases of mitochondrial DNA, Ann. Rev. Biochem. 61 (1992) 1175–1212.
[15] D.C. Wallace, Mouse models for mitochondrial disease, Am. J. Med. Genet. 106 (2001) 71–93.
[16] C.M. Wu, T. Matsuoka, M. Takemitsu, Y. Goto, I. Nonaka, An experimental model of mitochondrial myopathy: germanium-induced myopathy and coenzyme Q10 administration, Muscle Nerve 15 (1992) 1258–1264.
[17] T. Yamasoba, Y. Oka, K. Tsukuda, M. Nakamura, K. Kaga, Auditory findings in patients with maternally inherited diabetes and deafness harboring a point mutation in the mitochondrial transfer $RNA^{Leu(UUR)}$ gene, Laryngoscope 106 (1996) 49–53.
[18] T. Yamasoba, M. Suzuki, K. Kaga, Influence of chronic kanamycin administration on basement membrane anionic sites in the labyrinth, Hear Res. 102 (1996) 116–124.
[19] T. Yamasoba, J. Schacht, F. Shoji, J.M. Miller, Attenuation of cochlear damage from noise trauma by an iron chelator, a free radical scavenger and glial cell line-derived neurotrophic factor in vivo, Brain Res. 815 (1999) 317–325.
[20] T. Yamasoba, K. Tsukuda, Y. Oka, T. Kobayashi, K. Kaga, Cochlear pathology associated with mitochondrial $tRNA^{Leu(UUR)}$ gene mutation, Neurolog1 52 (1999) 1705–1707.

Cell Tissue Res
DOI 10.1007/s00441-006-0157-9

REGULAR ARTICLE

Tatsuya Yamasoba · Kenji Kondo

Supporting cell proliferation after hair cell injury in mature guinea pig cochlea in vivo

Received: 4 October 2005 / Accepted: 4 January 2006

Abstract In cold-blooded animals, lost sensory hair cells can be replaced via a process of regenerative cell proliferation of epithelial supporting cells. In contrast, in mammalian cochlea, receptor (hair) cells are believed to be produced only during embryogenesis; after maturity, sensory or supporting cell proliferation or regeneration are thought to occur neither under normal conditions nor after trauma. Using bromodeoxyuridine (BrdU) as a proliferation marker, we have assessed cell proliferation activity in the mature organ of Corti in the cochlea of young guinea pigs following severe damage to the outer hair cells induced by kanamycin sulfate and ethacrynic acid. Although limited, we have found BrdU-labeled nuclei in the regions of Deiters cells when BrdU is given for 3 days or longer. When BrdU is given for 10 days, at least one labeled nucleus can be observed in the organ of Corti in approximately half of the ears; proliferating cells typically appear as paired daughters, with one nucleus being displaced away from the basement membrane to the position expected of the hair cells. Double-staining with antibodies to cytokeratin, vimentin, and p27 have shown that the BrdU-labeled nuclei are located in cells phenotypically similar to Deiters cells. Most of the uptake of BrdU occurs 3–5 days following ototoxic insult, and the number of BrdU-labeled cells does not decrease until 30 days following insult. These findings indicate that Deiters cells in the mature mammalian cochlea maintain a limited competence to re-enter the cell cycle and proliferate after hair cell injury, and that they can survive at least for 1 month.

Keywords Cochlea · BrdU · p27 · Deiters cell · Hair cell · Regeneration · Guinea pig

This work was supported by the Ministry of Health, Labour, and Welfare, Japan (grants 12120101, 15110201) and by the Ministry of Education, Culture, Sports, Science, and Technology, Japan (grant 13470357) to T.Y.

T. Yamasoba (✉) · K. Kondo
Department of Otolaryngology and Head and Neck Surgery,
University of Tokyo,
Hongo 7-3-1, Bunkyo-ku,
Tokyo, 113-8655, Japan
e-mail: tyamasoba-tky@umin.ac.jp
Tel.: +81-3-58008924
Fax: +81-3-38149486

Introduction

Sensory receptors (hair cells) in the mammalian ear are located in the cochlear organ of Corti (OC) and in the vestibular sensory epithelia of the saccular macula, the utricular macula, and the cristae of the three semicircular canals. Two types of hair cells have been found in the OC: the inner (IHCs) and outer (OHCs) hair cells. The human cochlea possesses approximately 3,500 IHCs and approximately 12,000 OHCs. The IHCs are arranged in a single row and receive approximately 95% of their afferent innervation from the acoustic nerve. The OHCs are mostly arranged in three rows and contain a motile protein that induces contraction with stimulation and finely tune the response of the basilar membrane in order to determine the sharpness of the traveling wave generated by sound stimulation (Slepecky 1996). Hair cells in the mammalian OC are believed to be formed during a limited period of embryonic development, and after maturity, they are not thought to be replaced when they die (Ruben 1967; Bermingham-McDonogh and Rubel 2003). In humans, auditory hair cells can be damaged and lost as a consequence of acoustic trauma, treatment with ototoxic agents, infections, autoimmune pathologies, genetic susceptibilities, or as a part of the aging process. The loss of auditory hair cells in the human cochlea is a leading cause of permanent hearing deficits, currently affecting an estimated 600 million worldwide.

Lineage studies have shown that sensory hair cells and supporting cells arise from common progenitors in the inner ear (Lang and Fekete 2001). In cold-blooded animals, lost sensory hair cells can be quickly replaced via a process of regenerative cell proliferation of epithelial supporting

cells, which re-enter the cell cycle after hair cell injury (Corwin and Cotanche 1988; Ryals and Rubel 1988; Stone and Cotanche 1994; Bhave et al. 1995; Stone et al. 1999; Stone and Rubel 2000). A more limited regenerative response also has been observed in the damaged vestibular organs of mammals in which the reoccurrence of hair cells also reflects cell proliferation; this is most readily observed after treatment with mitogenic growth factors (Forge et al. 1993; Rubel et al. 1995; Li and Forge 1997; Kuntz and Oesterle 1998). Hair cell proliferation in the mammalian vestibular sensory epithelium encourages the expectation that a similar regeneration via cell proliferation may be possible in the mature mammalian cochlea after hair cell injury. Indeed, one controversial report suggests that in vitro retinoic acid can induce regeneration of auditory hair cells in ototoxic-poisoned rat OC explants (Lefebvre et al. 1993); however, other researchers have failed to confirm this finding (Chardin and Romand 1995). Although intensively sought, no evidence of cell proliferation has been observed to date in the postnatal mammalian OC (Ruben 1967; Roberson and Rubel 1994; Yamasoba et al. 2003; Bermingham-McDonogh and Rubel 2003). In part, this may reflect a limitation in the techniques used in these previous studies, which are largely based on the sectioning of the OC. Thus, labeled cells expressing the used proliferation marker may have been missed in the sectioned cochlea, in which it is impossible to observe all cells in the OC throughout the cochlea. We have therefore applied a surface preparation technique that has allowed us to observe the auditory sensory epithelium throughout the injured cochlea in a search to detect single bromodeoxyuridine (BrdU)-labeled cells.

Materials and methods

Animals

We employed 120 young albino guinea pigs (250–350 g) that had normal baseline auditory brainstem response (ABR) thresholds at 4, 8, and 20 kHz within the normal laboratory range.

Experimental protocol

The first aim of this study was to assess cell proliferation in the OC following hair cell injury. Ten animals that were deafened by systemic administration of kanamycin sulfate (KM) and ethacrynic acid (EA) on day 1 were given BrdU daily for 10 days from day 2 through day 11 and killed on day 12, 12 h following the last BrdU injection. This paradigm was set to exclude the possibility of the detection of dying cells that could passively take up BrdU. The OC was stained with antibodies to BrdU and observed under confocal laser microscopy. Eight control animals that were not deafened but that were given BrdU similarly for 10 days were also killed to investigate whether mitosis occurred in the normal OC (n=5) and for negative histological controls (n=3). The second aim, if BrdU-labeled cells were found, was to identify the type of cells labeled and to define the time window of their occurrence and the duration of their survival. Forty deafened animals were given BrdU daily for 10 days, from day 2 (following KM+EA) through day 11, and killed on day 12, 12 h following the last BrdU injection. In 10 of these animals, BrdU-labeled cells were made visible by the reaction to diaminobenzidine (DAB), and the surface and lateral views of the OC were examined under Nomarski optics at the light microscope level and by transmission electron microscopy (TEM). The remaining 30 animals were double-stained with antibodies to BrdU and p27 (n=10), cytokeratins (n=10), or vimentin (n=10). An additional 12 undeafened animals served as negative histological controls (n=3 each). To determine the timing of S-phase entry in the OC following hair cell injury, 40 animals given BrdU daily from day 2 until days 3, 4, 6, or 8 (n=10 each) were killed 12 h after the last BrdU injection (i.e., on days 4, 5, 7, or 9, respectively). Finally, to determine whether BrdU-labeled cells could survive for 1 month, 10 deafened animals were given BrdU for 10 days from day 2 through day 11 and killed on day 31.

The experimental protocol was approved by the University Committee for the Use and Care of Animals at the University of Tokyo and conformed to NIH Guidelines for the Care and Use of Laboratory Animals.

Deafening with KM and EA and BrdU injection

On day 1, experimental animals were given a single dose of KM (Meiji, Japan; 400 mg/kg, s.c.) and, 2 h later, under general anesthesia induced by intramuscular xylazine hydrochloride at 10 mg/kg (Bayer, Germany) and ketamine hydrochloride at 40 mg/kg (Sankyo, Japan)], they were prepared for cannulation of the jugular vein and injected with EA (50 mg/kg, i.v.), as previously reported (West et al. 1973). BrdU (Sigma, USA) dissolved in sterilized saline (10 mg/ml) was injected (100 mg/kg per injection, i.p.) twice each day at 12-h intervals from day 2 through day 11. The first injection of BrdU was given on day 2, 12 h following the administration of EA.

ABR measurement

Pure-tone (4, 8, and 20 kHz) ABRs were measured for both ears, 3 days after arrival (before deafening with KM and EA) in all animals and 3 days after deafening (on day 4) in all deafened animals. The method of ABR measurement was as described previously (Yamasoba et al. 1999). In brief, animals were anesthetized with a mixture of xylazine hydrochloride (10 mg/kg, i.m.) and ketamine hydrochloride (40 mg/kg, i.m.), and needle electrodes were placed subcutaneously at the vertex (active electrode), beneath the pinna of the measured ear (reference electrode), and beneath the opposite ear (ground). The stimulus duration was 15 ms, the presentation rate 11/s, and the rise/fall time

1 ms. Responses of 1024 sweeps were averaged at each intensity level (5 dB steps) to assess threshold. Threshold was defined as the lowest intensity level at which a clear reproducible waveform was visible in the trace. When an ABR waveform could not be evoked, threshold was assumed to be 5 dB greater than the maximum intensity produced by the system (105 dB SPL). Threshold shifts were calculated by subtracting baseline thresholds from those on day 4.

Immunocytochemistry

Animals were killed under deep anesthesia with xylazine and ketamine (as above), and the cochleae from both ears of each animal were perfused intrascalarly with 4% paraformaldehyde in 0.1 M phosphate-buffered saline (PBS) at pH 7.4 and immersed in the same fixative overnight at 4°C. The cochleae were then rinsed in 0.1 M PBS, and the surface of the OC was prepared by removing the otic capsule and tectorial membrane. The dissected specimens were incubated in methanol at −20°C for 20 min, immersed in 2 N HCl for 30 min, and preincubated in 4% normal goat serum in TRIS-buffered saline containing Tween 20 (TBS/T). For labeling with antibodies against p27, cytokeratins, or vimentin, the dissected specimens first were immersed in antigen retrieval solution (DAKO, USA) and microwaved at 95°C for 20 min. The specimens were then incubated overnight at room temperature in a solution containing primary antibodies. After several rinses, these specimens were incubated overnight at room temperature in a solution containing secondary antibodies. After several rinses, each turn of the cochlea was dissected out and mounted on glass slides with Prolong Antifade Kit (Molecular Probes, The Netherlands) and observed under a confocal laser scanning microscope (Axioskop MOT PLUS, Zeiss, Germany). The primary antibodies used were monoclonal rat anti-BrdU (1:500; Bitotech House, UK), monoclonal mouse anti-p27 (sc-1641, 1:200; Santa Cruz Biotechnology, USA), monoclonal mouse anti-pan-cytokeratin (clone PCK-26, 1:200; Sigma, USA), and monoclonal mouse anti-vimentin (clone V9, 1:50; Sigma), and secondary antibodies were fluorescein-isothiocyanate-conjugated affinity-purified goat anti-rat IgG (1:200; Molecular Probes) and rhodamin-conjugated affinity-purified goat anti-mouse IgG (1:200; Molecular Probes). For immunohistochemically negative controls, primary antibodies were omitted from the staining procedure.

Staining with antibodies to cytokeratin and vimentin was chosen because of the presence of both of these in the supporting cells, including the inner pillar cells and Deiters cells (DCs), but not in the hair cells in the mature guinea pig cochlea. Cytokeratins are present in the apical domain at the reticular lamina and in the basal domain near the basilar membrane in the supporting cells in normal cochlea and fill the expanded apical portions of the DCs in ototoxically damaged cochlea (Oesterle et al. 1990; Raphael and Altschuler 1991). Vimentin immunostaining is present in the cytoplasm of the third-row DCs, in the perinuclear region of the first-row and second-row DCs, and in the apical portion of the inner pillar cells. In general, vimentin is absent in the phalangeal scar when hair cells are destroyed by intense noise or ototoxic agents (Oesterle et al. 1990; Raphael and Altschuler 1991). Staining with antibodies to p27 was chosen because of the expression of this protein in the nuclei of the supporting cells of the OC (Chen and Segil 1999; Chen et al. 2002; Endo et al. 2002).

Observation of sections cut perpendicular to the basilar membrane

The dissected cochlear sensory epithelia were incubated with 3% H_2O_2 in methanol at −20°C for 30 min, immersed in 2 N HCl for 30 min, rinsed in PBS, and then incubated overnight at room temperature in a solution containing mouse monoclonal antibody to BrdU (Clone Bu20a; 1:500; DAKO, Denmark). After several rinses, these specimens were incubated overnight with a peroxidase-conjugated secondary antibody (Histofine, simple stain PO Max [Multi], Nichirei, Japan). They were then rinsed several times and allowed to react with DAB (Histofine, simple stain DAB; Nichirei, Japan). Each turn of the cochlea was mounted on a glass slide with aqueous/dry mounting medium (Crystal/mount, Biomeda, USA) and observed by Nomarski optics to detect BrdU-labeled nuclei in the OC. Turns including BrdU-labeled nuclei in the OC were then postfixed in 1% osmium tetroxide for 2 h, dehydrated in a graded alcohol series, and embedded in Epoxy resin. Consecutive sections of the embedded specimens, which were approximately 1 μm thick and perpendicular to the basilar membrane, were obtained, counterstained with toluidine blue, mounted on glass slides, and observed under Nomarski optics. Ultrathin sections of the specimens containing BrdU-labeled nuclei were then obtained, stained with uranyl acetate and lead citrate, and observed by TEM (H-800, Hitachi, Japan). The normal OC in three undeafened animals was processed similarly and served as a control.

Results

ABR findings in deafened animals

In all of the deafened animals, ABR measurement performed on day 4 showed significant increases of ABR thresholds, compared with the predeafening baseline measure. The mean threshold shifts (±SD) were 53±14, 62±18, and 68±14 dB at 4, 8, and 20 kHz, respectively. None of the animals showed ABR threshold shifts smaller than 30 dB at any frequencies examined.

Detection of BrdU-labeled cells in the OC in deafened animals given BrdU for 10 days

By 10 days following administration of KM and EA, the OHCs were destroyed nearly totally in the basal and second turns, moderately to severely in the third turn, and mildly in the apical turn, whereas almost all the IHCs and supporting cells throughout the OC remained intact. When lost, the OHCs were replaced by a phalangeal scar (Fig. 1a,j). This finding and the extent of ABR threshold shifts were similar

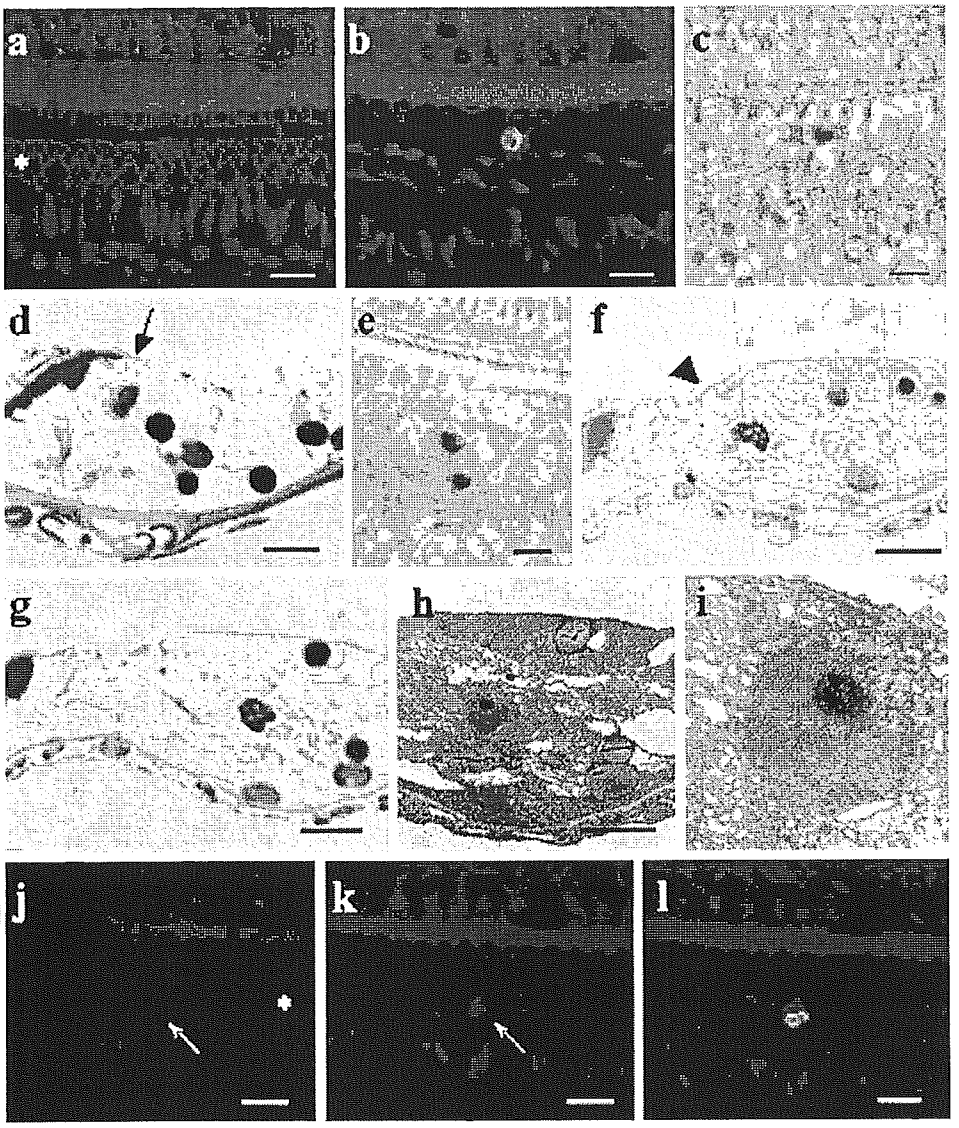

Fig. 1 **a–i** Organ of Corti (OC) of deafened animals given BrdU for 10 days. **a** In the apical surface of a whole-mount surface preparation of the OC, one inner hair cell is missing and all the outer hair cells (OHCs) are replaced by phalangeal scars (*asterisk*). **b** Below the scar shown in **a**, a single BrdU-labeled nucleus is observed in the first-row Deiters cell (DC). **c** An isolated single BrdU-labeled nucleus in the region of the first-row DCs in a whole-mount surface preparation of the OC. **d** Lateral view of the specimen shown in **c** demonstrates a BrdU-labeled cell located at a level normally occupied by the OHCs, with its superior portion extending to the reticular lamina (*arrow*) but containing no cuticular plate. **e** BrdU-labeled nuclei located in the region of second-row DCs in a whole-mount surface preparation of the OC. **f**, **g** Lateral views of specimen shown in **e** demonstrating labeled nucleus (**g**) located at a level normally occupied by nuclei of DCs and a second nucleus (**f**) nearer the reticular lamina. The superior portion of the latter reaches to the reticular lamina (*arrowhead*). **h**,**i** Low (**h**) and high (**i**) magnification transmission electron micrographs of the section shown in **g** demonstrating that the BrdU-labeled nucleus shows no sign of apoptosis. **j–l** The OC of deafened animals given BrdU for 5 days. **j** In the apical surface of a whole-mount surface preparation of the OC, all the OHCs are replaced by phalangeal scars (*asterisk*). The phalangeal scar of the cell containing BrdU-positive nuclei shown in **l** is indicated (*arrow*). **k** Approximately 6 μm below the section shown in **j**. DCs are present and exhibit expansion of their phalangeal processes (*arrow* phalangeal process of the cell containing BrdU-positive nuclei shown in **l**). **k** Approximately 12 μm below the section shown in **j**. BrdU-positive segregating daughter nuclei are present in the second-row DC. *Bars* 10 μm

to those reported by Izumikawa et al. (2005). In these animals, BrdU-labeled cells were frequently seen in tissues outside of the OC, such as fibroblasts and red blood cells in capillaries beneath the basilar membrane (data not shown). This staining, outside the OC, was also observed in undeafened controls, although the number of BrdU-labeled cells outside the OC was significantly smaller in controls compared with animals treated with KM and EA, as previously observed (Yamasoba et al. 2003). The BrdU staining outside the OC served as an internal positive control, ensuring that the BrdU, its antibody, and the secondary markers had reached the cochlea. Surprisingly, at least one BrdU-labeled nucleus was observed in the OC in 11 (55%) of 20 ears (Figs. 1b, 2); the number of BrdU-labeled nuclei ranged from 0 to 10 (3.6±3.1) per ear. BrdU-labeled nuclei were observed beneath the scar, most commonly in the regions of the first-row and second-row DCs and occasionally in the regions of the third-row DCs. Only a few labeled nuclei were observed in the regions of the outer pillar cells and Hensen cells. Most of BrdU-labeled nuclei were located within cells that demonstrated an upper portion projecting to the reticular lamina. Approximately one-third of BrdU-labeled nuclei were closely located, as pairs, whereas the remaining two-thirds were isolated, as single nuclei. Clusters of more than two labeled cells were not observed. BrdU-labeled nuclei were commonly observed in the lower three turns of the cochlea (Fig. 2), probably because the OHCs were damaged more severely in these turns. In control animals, no BrdU-labeled nuclei were observed within the normal OC. When the primary antibody was omitted from the immunohistochemical staining procedure, no labeled nuclei were present in any of the tissues examined (data not shown).

Lateral view of the BrdU-labeled cells in the OC

Lateral views of the OC demonstrated that BrdU-labeled nuclei were located commonly in the mid regions, at a level normally occupied by the nuclei of the DCs (Fig. 1e–i), and in some cases more apically (i.e., toward the reticular lamina), approximating the level normally occupied by the nuclei of the OHCs (Fig. 1c,d). The apical portions of cells containing BrdU-labeled nuclei were commonly extended to the reticular lamina but had no cuticular plate. Ultrathin sections of these specimens showed that all organelles were somewhat compromised by technical artifacts reflecting the use of 4% paraformaldehyde alone and repeated mounting. These degenerative changes were observed in all cells of the OC and in both control (data not shown) and experimental material, indicating that they were not drug-induced damage. We found no clear indication of apoptosis, such as nuclear condensation (Fig. 1h,i), in this material. However, given the BrdU-induced damage (artifacts) to nuclear structures, it waa difficult to conclude that apoptotic processes were not involved.

Double-staining with BrdU and p27, cytokeratin, or vimentin

Labeling with antibodies against p27 showed that the protein was expressed only in supporting cells and not in hair cells in the normal controls (data not shown), as previously reported (Chen and Segil 1999; Chen et al. 2002; Endo et al. 2002). In the deafened animals, BrdU-labeled nuclei in the OC were also labeled with p27 (Fig. 3a–c), and cytokeratins filled the expanded apical portions of DCs (Fig. 3d–f). Vimentin strongly labeled the cytoplasm of the third-row DCs and inner pillar cells and more faintly the perinuclear regions in the first-row and second-row DCs (Fig. 3g–i). The pattern of staining of these intermediate filaments was similar to that previously observed in the damaged cochlea (Oesterle et al. 1990; Raphael and Altschuler 1991). BrdU-labeled nuclei were located beneath the cytokeratin-positive apical portion of the DCs and in vimentin-positive cytoplasm in the DCs (Figs. 2, 3d–i). Vimentin was more strongly stained in the perinuclear regions of the first-row and second-row DCs labeled by BrdU compared with those unlabeled by BrdU. When two paired BrdU-labeled nuclei were found, one nucleus was commonly located in the inferior portion of

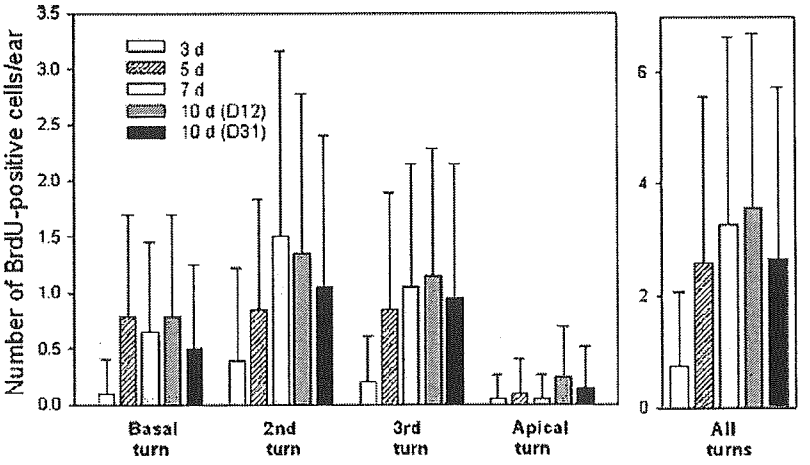

Fig. 2 Number (average±SD) of BrdU-labeled nuclei in the basal, second, third, and apical turns and the sum of these in animals deafened by administration of kanamycin sulfate and ethacrynic acid on day 1 and given BrdU from day 2 for 3 (n=10), 5 (n=10), 7 (n=10) or 10 (n=20) days. Animals given BrdU for 7 days or less were killed 12 h after the last BrdU injection, and those given BrdU for 10 days were killed on day 12, 12 h after the last BrdU injection (n=10) or on day 31 (n=10)

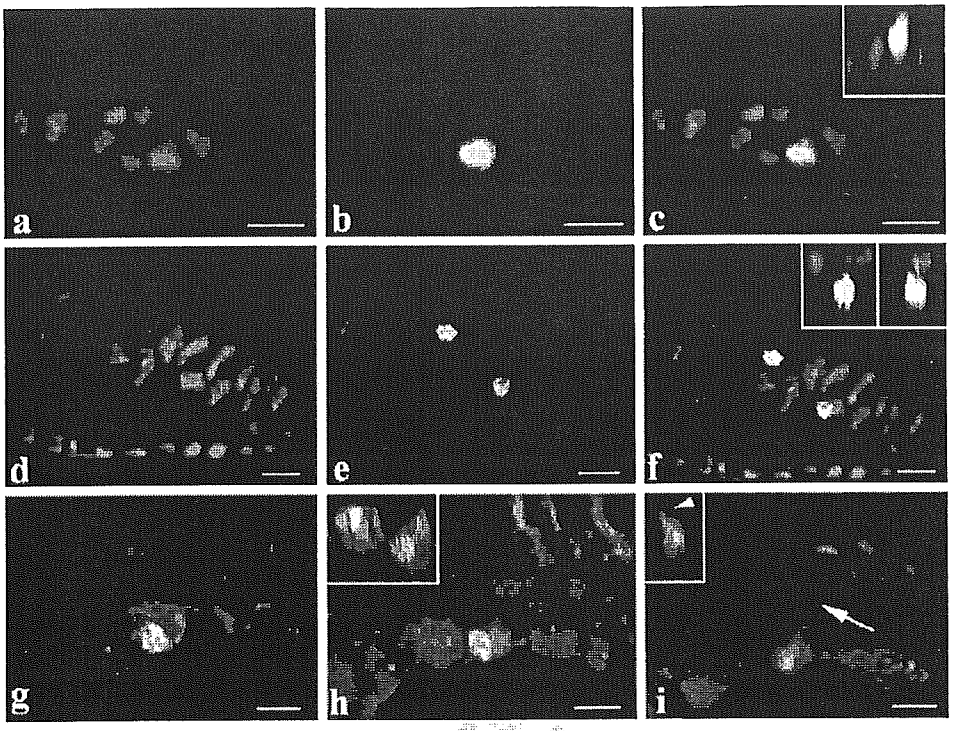

Fig. 3 Double-staining with antibodies against BrdU and p27 (**a–c**), cytokeratins (**d–f**), or vimentin (**g–i**) in whole-mount surface preparations of the OC of deafened animals given BrdU for 10 days. **a** Nuclei of the first-row and second-row DCs are labeled with p27. **b** One BrdU-labeled nucleus is present in a second-row DC. **c** The merged view and ortho-image of these slices (*inset*) show that the BrdU-labeled nucleus is also labeled with p27. **d** The expanded apical portions of the DCs are labeled with cytokeratins. **e** Two BrdU-labeled nuclei are present in the regions of first-row and second-row DCs. **f** The merged view and ortho-images of these slices (*insets*) show that BrdU-labeled nuclei are located beneath the apical portions of the DCs. **g** One BrdU-labeled nucleus in the first-row DC is present slightly beneath the reticular lamina. Vimentin is stained in the regions around the BrdU-labeled nuclei. **h** Another BrdU-labeled nucleus is present in vimentin-positive cytoplasm of an adjacent DC (*inset* ortho-image of these slices). **i** Approximately 6 μm below the section shown in **h**, vimentin is more faintly stained in the cytoplasm of DCs unlabeled by BrdU. The phalangeal process (*arrow*; *arrowhead* in *inset*) obliquely projects from the BrdU-labeled DC. *Bars* 10 μm

vimentin-positive cytoplasm of the DC and the second in the more apical portion of the neighboring DCs (Fig. 3g–i).

Timing of appearance of BrdU-labeled cells following injection with KM and EA

Because a total of 20 injections of BrdU over a 10-day period resulted in only the limited uptake of BrdU in the OC after ototoxic insults, we considered it impossible to identify the timing of S phase after hair cell injury by a single injection of BrdU. We therefore adopted a strategy of applying cumulative BrdU, by injections over different courses of treatment. BrdU-labeled nuclei were absent in the OC in all animals given BrdU for only 2 days. A small number of the BrdU-labeled nuclei were first detected in the OC of animals given BrdU for 3 days. The number of BrdU-labeled nuclei significantly increased when BrdU was given for 5 days and did not significantly change thereafter (Fig. 2). We also found a DC that contained segregating BrdU-positive daughter nuclei in an animal given BrdU for 5 days (Fig. 1j–l).

Survival of BrdU-labeled cells

When animals were given BrdU for 10 days and killed on day 31, almost all the OHCs were missing and replaced by a phalangeal scar in the second and third turns, whereas damage to the OHCs in the apical turn was mild to moderate. In the basal turn, no OHCs were observed in any of the animals, and the OC was commonly collapsed. At least one BrdU-labeled nucleus was observed in the OC in 10 (50%) out of 20 ears. The number of BrdU-labeled nuclei ranged from 0 to 8 (2.7±3.1) per ear, which was not significantly different from that (3.6±3.1 per ear) in animals given BrdU for 10 days and killed on day 12 (Fig. 2). These findings indicated that BrdU-labeled cells could survive at least for 1 month.

Discussion

Following administration of KM and EA, we observed limited numbers of BrdU-labeled nuclei in the regions of the DCs in the mature OC of the young guinea pig. BrdU-